

## Relation between cancer cellularity and apparent diffusion coefficient values using diffusion-weighted magnetic resonance imaging in breast cancer

Miho I. Yoshikawa · Shozo Ohsumi · Shigenori Sugata

Masaaki Kataoka · Shigemitsu Takashima

Teruhito Mochizuki · Hirohiko Ikura · Yutaka Imai

Received: September 25, 2007 / Accepted: December 10, 2007

© Japan Radiological Society 2008

### Abstract

**Purpose.** The purpose of this study was to examine the relation between cancer cellularity and the apparent diffusion coefficient (ADC) value using diffusion-weighted magnetic resonance imaging in breast cancer.

**Materials and methods.** The subjects were 27 women who had undergone operation for breast cancer. There were 27 breast cancer lesions, 24 of which were invasive ductal carcinoma (IDC) and 3 of which were noninvasive ductal carcinoma (NIDC).

**Results.** The mean ADC values of IDC, NIDC, and normal breasts were  $1.07 \pm 0.19 \cdot 10^{-3}$ ,  $1.42 \pm 0.17 \cdot 10^{-3}$ , and  $1.96 \pm 0.21 \cdot 10^{-3} \text{ mm}^2/\text{s}$ , respectively. The mean ADC

values of IDC and NIDC were significantly different from that of normal breasts ( $P < 0.001$  each). The mean ADC values were also significantly different between IDC and NIDC ( $P < 0.001$ ). There was no correlation between the ADC value and cancer cellularity.

**Conclusion.** The mean ADC values for breast cancer were significantly different from that of normal breasts. The mean ADC value for breast cancer did not significantly correlate with cancer cellularity but did correlate with histological types.

**Key words** Breast cancer · MRI · Diffusion-weighted imaging · Cellularity · Apparent diffusion coefficient value

M.I. Yoshikawa (✉) · H. Ikura

Department of Radiology, Tokai University School of Medicine, Tokai University Hachioji Hospital, 1838 Ishikawa, Hachioji, Tokyo 192-0032, Japan  
Tel. +81-42-639-1111; Fax +81-42-639-1112  
e-mail: mihoyoshikawa@yahoo.co.jp

S. Ohsumi · S. Takashima

Department of Breast Surgery, National Hospital Organization Shikoku Cancer Center, Matsuyama, Japan

S. Sugata · M. Kataoka

Department of Radiology, National Hospital Organization Shikoku Cancer Center, Matsuyama, Japan

T. Mochizuki

Department of Diagnostic and Therapeutic Radiology, Ehime University Graduate School of Medicine, Toon, Japan

Y. Imai

Department of Radiology, Tokai University School of Medicine, Isehara, Japan

### Introduction

Diffusion is a physical process that is used to describe the motion of water molecules, known as Brownian motion. Diffusion-weighted magnetic resonance imaging (DW-MRI) is the only method to measure molecule diffusion *in vivo*.<sup>1</sup> DW-MRI provides information on microstructure, such as tissue cellularity, which has been shown to be an important index of tumor grade,<sup>2–4</sup> and local tissue architecture, which is a sensitive early indicator of abnormality.<sup>5,6</sup>

DW-MRI has been applied to a variety of intracranial lesions, including acute cerebral infarcts, tumors, and demyelinating diseases.<sup>7,8</sup> Application of DW-MRI to the breast had been limited by movement artifact (i.e., breathing and heartbeats), but the usefulness of identifying and diagnosing the features of thoracoabdominal local lesions by DW-MRI using echo planar imaging

(EPI) has been reported since short-time acquisition using EPI was developed.<sup>9–19</sup>

The purpose of this study was to examine the relation between cellularity and the apparent diffusion coefficient (ADC) value using DW-MRI in breast cancer.

## Materials and methods

### Subjects

The subjects were 27 women who had undergone an operation for breast cancer (ages 28–72 years, mean 53.4 years); they had a total of 27 breast cancer lesions. These women had undergone DW-MRI before surgery at the Shikoku Cancer Center between October 2003 and March 2004. In total, 24 lesions were invasive ductal carcinoma (IDC) and 3 were noninvasive ductal carcinoma (NIDC). The mean size of the IDCs was 20 mm (9–30 mm), and the mean size of the NIDCs was 22 mm (8–35 mm). In all cases, no abnormality was found by palpation, mammography (MMG), or enhanced MRI in the other breast.

### MRI protocol

The instruments used were a 1.5 T MR (Intera 1.5T, Philips Healthcare Nederland, Eindhoven, the Netherlands), and a synergy body coil. Coronal sections were imaged by T1-weighted imaging (T1WI), T2-weighted imaging (T2WI), and diffusion-weighted imaging (DWI) in the prone position. With DWI, SE type EPI combining CHESS and SENSE was performed. After contrast imaging, three-dimensional (3D) coronal fat-suppressed T1-weighted images were acquired.

T1WI was performed using the following parameters: TR/TE 490/11 ms, NEX 2, slice thickness 4 mm, interslice gap 0, acquisition matrix 384 × 250, field of view (FOV) 28 cm. T2WI was performed using the following parameters: TR/TE 6082/100 ms, NEX 2, slice thickness 4 mm, interslice gap 0, acquisition matrix 448 × 292, FOV 28 cm.

For DWI, the axial image was acquired by SE type EPI combining CHESS and SENSE. Sensitizing diffusion gradients were applied sequentially in the x-, y-, and z-directions with b values of 0, 200, 400, 600, and 800 s/mm<sup>2</sup> using TR/TE 6238/90 ms, NEX 1, slice thickness 4 mm, interslice gap 0, bandwidth 2.4 kHz, acquisition matrix 128 × 77, FOV 28 cm, acquisition time 87 s. After DWI, a 3D scan by gadolinium (Gd)-enhanced fast gradient echo (Gd-EFGRE) was performed to identify the lesion accurately. All lesions were detected by Gd-EFGRE.

### Analysis of the apparent diffusion coefficient

The ADC values were calculated by the algorithm presented by the following equation.

$$\text{ADC} (\text{mm}^2\text{s}^{-1}) = 1/b_1 \times \ln[\text{IS}(b_0)/\text{IS}(b_1)]$$

IS ( $b_0$ ) and IS ( $b_1$ ) are signal densities in the region of interest (ROI) obtained by two gradient factors,  $b_0$  and  $b_1$ . To measure the signal intensity of the lesions, an ROI that was minimally smaller than the actual solid portion of the breast lesion was carefully placed to ensure that cystic or necrotic areas cleared on imaging were not included, and the mean ADCs were then obtained.

### Cancer cellularity analysis

Analysis of cancer cellularity was performed by utilizing a method essentially similar to the one used by Guo et al.<sup>12</sup> Initially, five slides (counterstained with hematoxylin and eosin) were obtained from different areas of the lesion in each tumor. One FOV (original magnification × 200) was randomly chosen from each slide and photographed for the eventual analysis of cancer cellularity. The films of the specimens were then scanned into a personal computer. Cancer cells were carefully labeled using black points by graphic software (Adobe Photoshop 7.0). The points were then counted with Scion Image Beta 4.03 software for Windows. Cancer cellularity and the mean ADCs were compared using simple linear regression analysis.  $P < 0.01$  was considered to indicate statistical significance.

## Results

The mean ADC values of the histological types were calculated. The mean ADC values for IDC, NIDC, and normal breasts were  $1.07 \pm 0.19 \times 10^{-3}$ ,  $1.42 \pm 0.17 \times 10^{-3}$ , and  $1.96 \pm 0.21 \times 10^{-3}$  mm<sup>2</sup>/s, respectively. The ADC values for IDC and NIDC were significantly different from that of normal breasts ( $P < 0.001$  each). Mean ADC values were also significantly different between IDC and NIDC (Table 1) ( $P < 0.001$ ).

We then examined the relation between cancer cellularity and the ADC using DW-MRI. There was no correlation between the ADC value and cancer cellularity (Fig. 1). For instance, two cases of IDC in Fig. 2 and NIDC in Fig. 3 showed approximately similar cancer cellularity. In a case of IDC in Fig. 2, the cellularity was 437 in a high magnification FOV with a low ADC value ( $0.83 \times 10^{-3}$  mm<sup>2</sup>/s). In a case of NIDC in Fig. 3, the cellularity was 391 in a high magnification FOV with a high

ADC value ( $1.36 \times 10^{-3} \text{ mm}^2/\text{s}$ ). On the other hand, two cases of IDC in Figs. 2 and 4 also showed approximately similar ADC values. In a case of IDC in Fig. 4, the cellularity was 1128 in a high magnification FOV with a low ADC value ( $0.98 \times 10^{-3} \text{ mm}^2/\text{s}$ ).

## Discussion

DW-MRI shows the Brownian movement of a water molecule and is the only method for measuring molecule diffusion in vivo.<sup>1</sup> DW-MRI provides information on microstructure such as tissue cellularity, which has been shown to be an important index of tumor grade,<sup>2–4</sup> and

**Table 1.** Mean apparent diffusion coefficients for the histological types

Histological type	No. of cases	Mean ADC ( $\times 10^{-3} \text{ mm}^2/\text{s}$ )
IDC	24	$1.07 \pm 0.19$
NIDC	3	$1.42 \pm 0.17$
Normal	27	$1.96 \pm 0.21$

ADC, apparent diffusion coefficient; IDC, invasive ductal carcinoma; NIDC, noninvasive ductal carcinoma

The mean ADCs for IDC, NIDC, and normal breasts were  $1.07 \pm 0.19 \times 10^{-3}$ ,  $1.42 \pm 0.17 \times 10^{-3}$ , and  $1.96 \pm 0.21 \times 10^{-3} \text{ mm}^2/\text{s}$ , respectively. The mean ADCs for IDC and NIDC were significantly different from that of normal breasts ( $P < 0.001$  each). Mean ADCs for IDC and NIDC were significantly different ( $P < 0.001$ )

local tissue architecture, which is a sensitive early indicator of abnormality.<sup>5,6</sup>

DW-MRI has recently been reported to be capable of identifying and diagnosing features of tumors in the breast. There are some reports about the ADC values of cancerous and normal breast.<sup>6,13–17</sup> Shinha and Lucas-Quesada<sup>6</sup> reported that the ADC values of cancerous

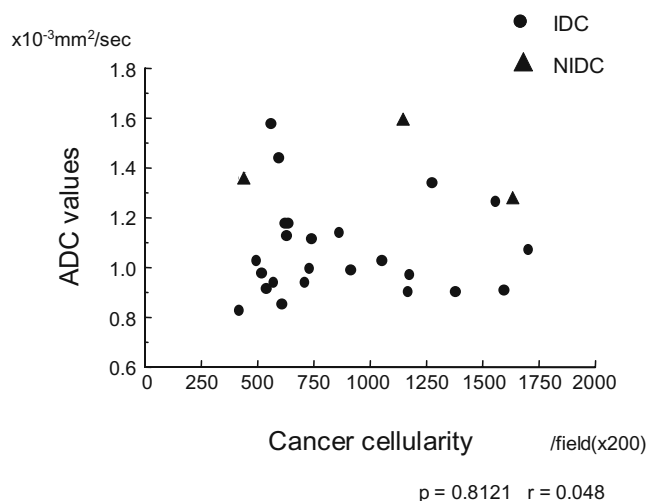


**Fig. 1.** Relation between cancer cellularity and the apparent diffusion coefficient (ADC) value for breast cancer. The mean ADC value of breast cancer did not significantly correlate with cancer cellularity, but it did correlate with histological type.  $P = 0.8121$ ,  $r = 0.048$ . IDC, invasive ductal carcinoma; NIDC, noninvasive ductal carcinoma

**Fig. 2.** Material from a 62-year-old patient with invasive ductal carcinoma that had a maximum diameter of 30 mm measured histologically. **A** On gadolinium-enhanced fast gradient echo (Gd-EFGRE), an irregular mass with a microlobulated margin and heterogeneous internal enhancement was seen. **B** On diffusion-weighted magnetic resonance imaging (DW-MRI), the enhanced area is depicted as hyperintense, with an ADC value of  $0.83 \times 10^{-3} \text{ mm}^2/\text{s}$ . **C** Histological specimen shows that the cancer cellularity of the tumor is 437 in a  $200 \times$  (high magnification) field of view

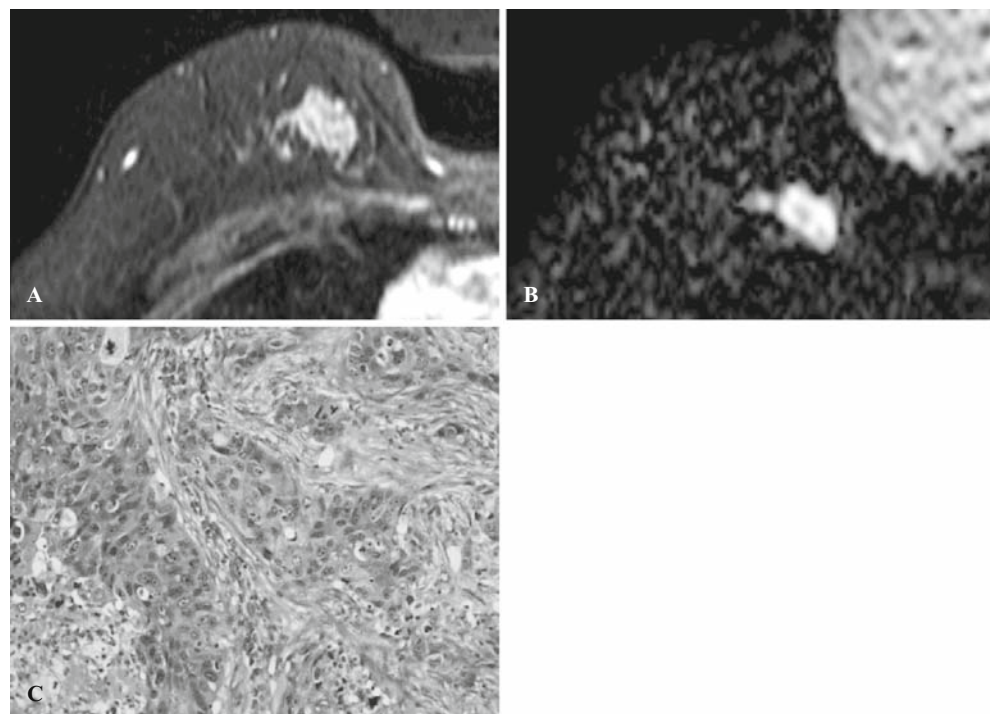


**Fig. 3.** Material from a 52-year-old patient with noninvasive ductal carcinoma that had a maximum diameter of 35 mm measured histologically. **A** On Gd-EFGRE, nonmass-like enhancement is regional and heterogeneous. **B** On DW-MRI, the enhanced area is depicted as hyperintense with an ADC value of  $1.36 \times 10^{-3} \text{ mm}^2/\text{s}$ . **C** Histological specimen shows that the cancer cellularity of the tumor is 391 in a  $200 \times$  (high magnification) field of view

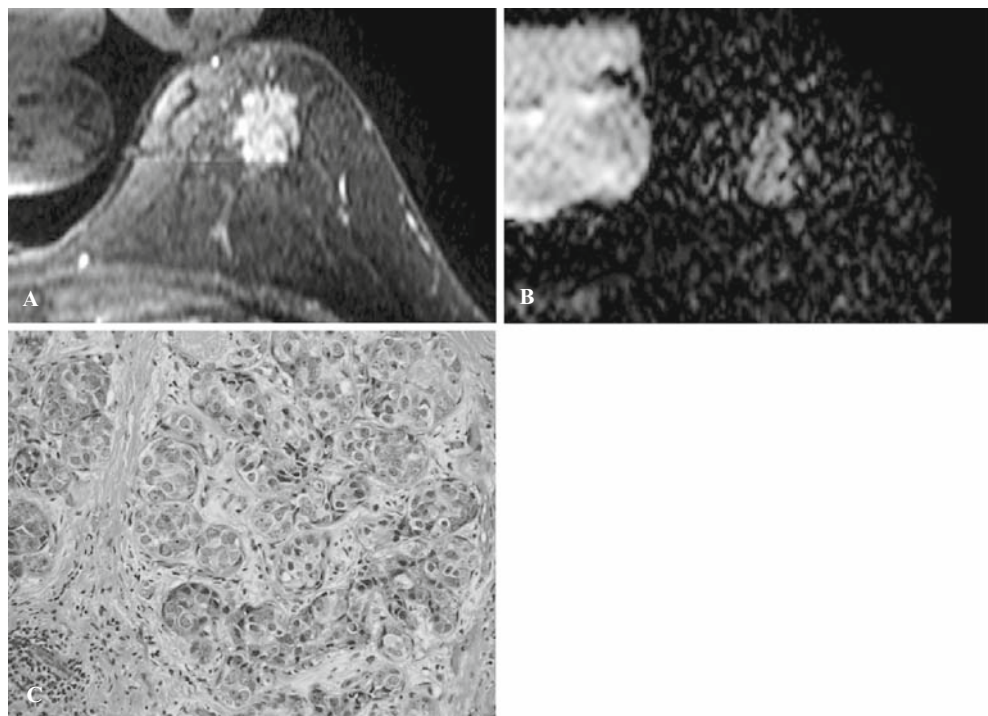
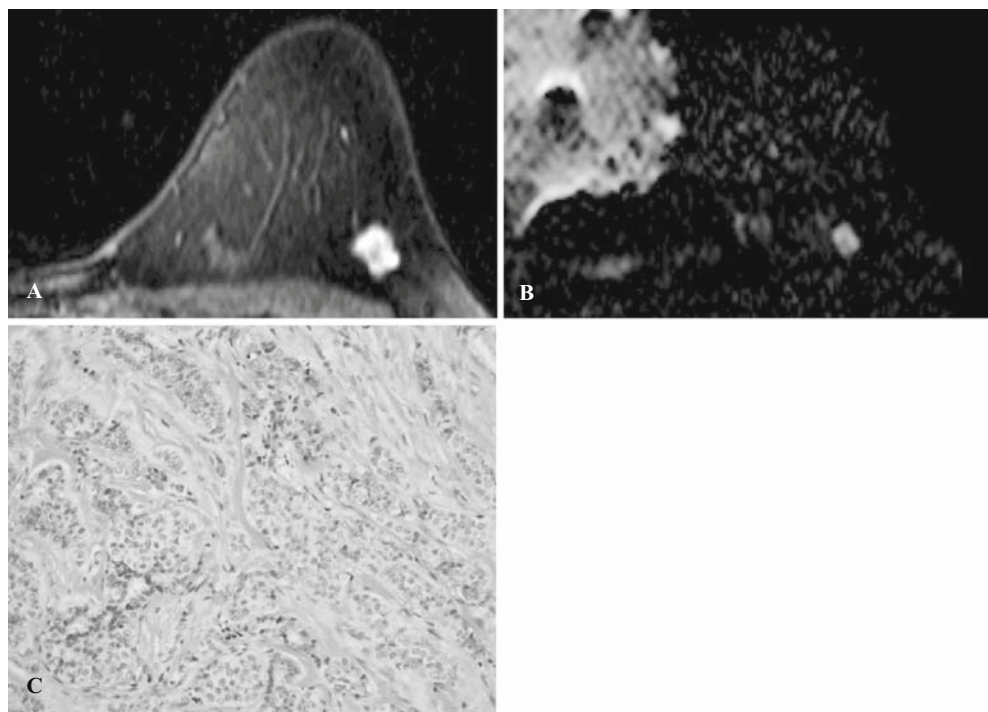


**Fig. 4.** Material from a 52-year-old patient with invasive ductal carcinoma that had a maximum diameter of 9 mm measured histologically. **A** Gd-EFGRE revealed a lobular mass with a circumscribed margin and dark internal septation. **B** On DW-MRI, the enhanced area is depicted as hyperintense with an ADC value of  $0.98 \times 10^{-3} \text{ mm}^2/\text{s}$ . **C** Histological specimen shows that the cancer cellularity of the tumor is 1128 in a  $200 \times$  (high magnification) field of view



and normal breasts were  $1.01 \pm 0.17 \times 10^{-3}$  and  $1.63 \pm 0.22 \times 10^{-3} \text{ mm}^2/\text{s}$ , respectively. A similar result was found in this study, but there was a small number of NIDCs (Table 1). The values for IDCs and NIDCs were significantly different from that of normal breasts ( $P < 0.001$  each). The mean ADC values were also signifi-

cantly different between IDCs and NIDCs ( $P < 0.001$ ). The mean ADC value of breast cancer correlated with the histological type.

In our study, the mean ADC values of breast cancer did not significantly correlate with cancer cellularity (Fig. 1). Squillaci et al.<sup>20</sup> reported that the mean ADC

value of renal tumors did not significantly correlate with tumor cellularity. In contrast, Sugahara et al.<sup>3</sup> reported that tumor cellularity correlated well with the minimum ADC value of gliomas. Guo et al.<sup>12</sup> reported that the mean ADCs of breast lesions, which were malignant and benign, correlated well with tumor cellularity; and their histological examinations showed the cellularity of malignant breast tumors to be hypercellular compared to that of benign tumors.<sup>21</sup> We speculate that ADC values depend on not only cancer cellularity but also histological type. Therefore, one of the factors on which the ADC value depends may be also the state of the stroma. It seems that it is necessary to examine the cellularity of the whole organization, which includes not only the cancer cells but also the stromal ingredient and area the cancer cell occupies.

## Conclusion

The ADC values of breast cancer were significantly different from that of normal breasts. Mean ADC values were also significantly different between IDCs and NIDCs. The mean ADC value for breast cancer did not significantly correlate with cancer cellularity but did correlate with the histological type.

## References

- Lebihan D, Turner R, Douek P, Patronas N. Diffusion MR imaging: clinical applications. *AJR Am J Roentgenol* 1992; 159:591–9.
- Ducatman BS, Emery ST, Wang HH. Correlation of histologic grade of breast carcinoma with cytologic features on fine-needle aspiration of the breast. *Mod Pathol* 1993;6: 539–43.
- Sugahara T, Korogi Y, Kochi M, Ikushima I, Shigematsu Y, Hirai T, et al. Usefulness of diffusion-weighted MRI with echo-planar technique in the evaluation of cellularity in gliomas. *J Magn Reson Imaging* 1999;9:53–60.
- Lyng H, Garaldseth O, Rofstad EK. Measurement of cell density and necrotic fraction in human melanoma xenografts by diffusion weighted magnetic resonance imaging. *Magn Reson Med*. 2000;43:828–36.
- Le Bihan D, Mangin JF, Poupon C, Clark CA, Pappata S, Molko N, et al. Diffusion tensor imaging: concepts and applications. *J Magn Reson Imaging* 2001;13:534–46.
- Shinha S, Lucas-Quesada F. In vivo diffusion-weighted MRI of the breast: potential for lesion characterization. *J Magn Reson Imaging* 2002;15:693–704.
- Warach S, Chien D, Li W, Ronthal M, Edelman RR. Fast magnetic resonance diffusion-weighted imaging of acute human stroke. *Neurology* 1992;42:1717–23.
- Lovblad KO, Laubach HJ, Baird AE, Curtin F, Schlaug G, Edelman RR. Clinical experience with diffusion-weighted MR in patients with acute stroke. *AJNR Am J Neuroradiol* 1998;19:1061–6.
- Ichikawa T, Haradome H, Hachiya J, Nitatori T, Araki T. Diffusion-weighted MR imaging with single-shot echo-planar imaging in the upper abdomen: preliminary clinical experience in 61 patients. *Abdom Imaging* 1999;24:456–61.
- Yamashita Y, Namimoto T, Mitsuzaki K, Urata J, Tsuchigame T, Takahashi M, et al. Mucin-producing tumor of the pancreas: diagnostic value of diffusion-weighted echo-planar MR imaging. *Radiology* 1998;208:605–9.
- Moteki T, Ishizuka H. Diffusion-weighted EPI of cystic ovarian lesions: evaluation of cystic contents using apparent diffusion coefficients. *J Magn Reson Imaging* 2000;12:1014–9.
- Guo Y, Cai ZI, Cai TQ, Guo YG, An NY, Ma L, et al. Differentiation of clinically benign and malignant lesions using diffusion-weighted imaging. *J Magn Reson Imaging* 2002;16: 172–8.
- Kuroki Y, Nasu K, Kuroki S, Murakami K, Hayashi T, Sekiguchi R, et al. Diffusion-weighted imaging of breast cancer with the sensitivity encoding technique: analysis of the apparent diffusion coefficient value. *Magn Reson Med Sci* 2004;3:79–85.
- Woodhams R, Matsunaga K, Kan S, Hata H, Ozaki M, Iwabuchi K, et al. ADC mapping of benign and malignant breast tumors. *Magn Reson Med Sci* 2005;4:35–42.
- Woodhams R, Matsunaga K, Iwabuchi K, Kan S, Hata H, Kuranami M, et al. Diffusion-weighted imaging of malignant breast tumors: the usefulness of apparent diffusion coefficient (ADC) value and ADC map for the detection of malignant breast tumors and evaluation of cancer extension. *J Comput Assist Tomogr* 2005;29:644–9.
- Kuroki-Suzuki S, Kuroki Y, Nasu K, Nawano S, Moriyama N, Okazaki M. Detecting breast cancer with non-contrast MR imaging: combining diffusion-weighted and STIR imaging. *Magn Reson Med Sci* 2007;6:21–7.
- Yoshikawa MI, Ohsumi S, Sugata S, Kataoka M, Takashima S, Kikuchi K, et al. Comparison of breast cancer detection by diffusion-weighted magnetic resonance imaging and mammography. *Radiat Med* 2007;25:218–3.
- Englander SA, Ulug AM, Brem R, Glickson JD, van Zijl PC. Diffusion imaging of human breast. *NMR Biomed* 1997;10: 348–52.
- Partridge S, McKinnon G, Henry RG, Hylton NM. Menstrual cycle variation of apparent diffusion coefficients measured in the normal breast using MRI. *J Magn Reson Imaging* 2001;14:433–8.
- Squillaci E, Manenti G, Cova M, Di Roma M, Miano R, Palmieri G, et al. Correlation of diffusion-weighted MR imaging with cellularity of renal tumors. *Anticancer Res* 2004; 24:4175–9.
- Ducatman BS, Emery ST, Wang HH. Correlation of histologic grade of breast carcinoma with cytologic features on fine-needle aspiration of the breast. *Mod Pathol* 1993;6: 539–43.